

Narrowband Interference Suppression for MIMO MB-OFDM UWB Communication Systems

Georgi Iliev

Department of Telecommunications
Technical University of Sofia
Sofia, Bulgaria
e-mail: gli@tu-sofia.bg

Zlatka Nikolova

Department of Telecommunications
Technical University of Sofia
Sofia, Bulgaria
e-mail: zvv@tu-sofia.bg

Vladimir Poulkov

Department of Telecommunications
Technical University of Sofia
Sofia, Bulgaria
e-mail: vkp@tu-sofia.bg

Miglen Ovtcharov

Department of Telecommunications
Technical University of Sofia
Sofia, Bulgaria
e-mail: miglen.ovcharov@jci.com

Abstract—Ultrawideband (UWB) systems show excellent potential benefits when used in the design of high-speed digital wireless home networks. The constantly-increasing demand for higher data transmission rates can be satisfied by exploiting both multipath- and spatial-diversity, using multiple-input multiple-output (MIMO) together with proper modulation and coding techniques. Unlike conventional MIMO OFDM systems, the performance of MIMO MB-OFDM UWB systems does not depend on the temporal correlation of the propagation channel although narrowband interference (NBI) is still a problem. In this paper we put forward a technique for suppressing NBI by the use of adaptive narrowband filtering. The method is compared experimentally with other algorithms for the identification and cancellation/suppression of complex NBI in OFDM single-band and multiband (MB) UWB systems. The study shows that the different schemes offer slightly differing performances, depending on the parameters of the MIMO UWB system. The proposed complex adaptive narrowband filtering technique is an optimal solution which offers a good balance between NBI suppression efficiency and computational complexity.

Keywords - Narrowband interference (NBI); Multiband orthogonal frequency-division multiplexing (MB-OFDM); Multiple-input multiple-output (MIMO); Ultrawideband (UWB); Variable complex filters; Adaptive complex filter banks.

I. INTRODUCTION

In recent years, ultrawideband (UWB) signals have been employed extensively in communications and ranging applications. Depending on how the available bandwidth of the system is used, UWB can be divided into two groups: single-band and multiband.

Conventional UWB technology is based on single-band systems and employs carrier-free communications [1]–[3]. It is implemented by directly modulating information into a sequence of impulse-like waveforms; support for multiple

users is by means of time-hopping or direct sequence spreading approaches.

The UWB frequency band of multiband UWB systems is divided into several sub-bands, with the bandwidth of each of them being at least 500 MHz [4] [5]. By interleaving the symbols across sub-bands, multiband UWB can maintain the power of the transmission as though a wide bandwidth were being utilized. The advantage of the multiband approach is that it allows the information to be processed over a much smaller bandwidth, thereby reducing overall design complexity as well as improving spectral flexibility and worldwide adherence to the relevant standards. In order to capture the multipath energy efficiently, the orthogonal frequency division multiplexing (OFDM) technique is used to modulate the information in each sub-band. The major difference with MB-OFDM, as opposed to more traditional OFDM schemes, is that the MB-OFDM symbols are not continuously sent on one frequency-band; instead they are interleaved over different sub-bands across both time and frequency. Multiple access of multiband UWB is enabled by the use of suitably-designed frequency-hopping sequences over the set of sub-bands.

Most UWB applications are used indoors, thus providing an excellent transmission environment for MIMO implementation. Moreover, the GHz center frequency of UWB systems makes the spacing between antenna array elements less critical. In consequence, the combination of UWB and MIMO technology becomes an effective method of achieving the very high data rates required for high-speed short-range communications. Multi-antenna UWB technology has been well-explored in conventional single-band UWB systems [6]–[8]. Conversely, research into multiband UWB systems employing multiple antennae is as yet not complete, so the full benefits of UWB-MIMO communications systems have therefore not been entirely explored.

The main difference between MIMO OFDM and MIMO MB-OFDM lies in the channel characteristics. The block diagram for MIMO MB-OFDM is shown in Figure 1.

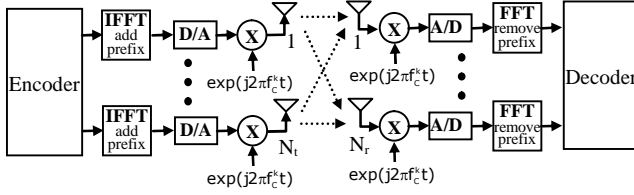


Figure 1. MIMO MB-OFDM UWB system.

In this paper, we look at UWB MIMO systems with MB-OFDM, a leading technology for many broadband communication systems [9]. Due to their relatively low transmission power, such systems are very sensitive to narrowband interference (NBI). Because of the spectral leakage effect caused by Discrete Fourier Transform (DFT) demodulation at the OFDM receiver, many subcarriers near the interference frequency suffer from serious Signal-to-Interference Ratio (SIR) degradation, which can adversely affect or even block communications [10].

The issue of NBI suppression in wideband OFDM systems is of primary importance in such systems and has been studied extensively in the last few years [11]. Two main types of approach are generally adopted. The first involves various frequency excision methods, whereby the affected frequency bins of the OFDM symbol are excised or their usage avoided [12]. The second approach is related to “cancellation techniques” which are aimed at eliminating or mitigating the effect of the NBI on the received OFDM signal [13]. In most cases, the degradation in a MIMO MB-OFDM-based receiver is beyond the reach of the frequency excision method when the SIR is less than 0 dB. Thus, mitigation techniques employing cancellation methods, one of which is based on complex adaptive filtering and the other on NBI identification and cancellation, are recommended as an alternative [14]-[17].

In this paper, a method for NBI cancellation based on adaptive complex digital filtering, using the Least Mean Squares (LMS) algorithm to adapt to the central frequency of the NBI [18], is presented and the method is compared to other mitigation techniques. The study shows that all schemes give different performances, depending on the parameters of the MB-OFDM MIMO UWB system, but the proposed method offers considerable benefits, including low computational complexity.

The rest of the paper is organized as follows: In Section II the adaptive filtering scheme using variable complex adaptive narrowband filter is considered. An adaptive complex notch filter bank for the cancellation/enhancement of multiple complex signals is also proposed. The simulation model for NBI suppression in UWB systems is described in Section III. Section IV presents the simulation results for NBI suppression in UWB channels and MIMO MB-OFDM systems. Finally, Section V concludes the paper.

II. NBI SUPPRESSION USING ADAPTIVE COMPLEX FILTERING

In comparison with the information wideband signal, the interference occupies a much narrower frequency band but has a higher-power spectral density [19]. On the other hand, the wideband signal usually has autocorrelation properties quite similar to those of AWGN (Adaptive Wide Gaussian Noise), so filtering in the frequency domain is possible.

A. Variable Complex Narrowband Digital Filter

The filtering process is carried out at the input of the OFDM demodulator by the use of a variable complex filter with independent tuning of the central frequency and bandwidth. This is then turned into an adaptive narrowband filter to be implemented in an OFDM receiver.

A variable complex bandpass (BP) first-order digital filter designated LS1 (Low Sensitivity) is designed [20] (Figure 2). The transfer functions of the LS1 section, all of BP type, are:

$$H_{RR}(z) = H_{II}(z) = \frac{\hat{\beta} + 2\hat{\beta}^2 \cos\theta z^{-1} + \hat{\beta}(2\hat{\beta} - 1)z^{-2}}{1 + 2(2\hat{\beta} - 1)\cos\theta z^{-1} + (2\hat{\beta} - 1)^2 z^{-2}}, \quad (1)$$

$$H_{RI}(z) = -H_{IR}(z) = \frac{2\hat{\beta}(1 - \hat{\beta})\sin\theta z^{-1}}{1 + 2(2\hat{\beta} - 1)\cos\theta z^{-1} + (2\hat{\beta} - 1)^2 z^{-2}}.$$

The composed multiplier $\hat{\beta}$ is $\hat{\beta} = \beta + 2\beta(\beta - 1)$.

The bandwidth can be tuned by trimming the single coefficient β , whereas θ controls the central frequency ω_0 .

This design of variable complex digital filter has two very important advantages: firstly, an extremely low passband sensitivity which offers resistance to quantization effects; secondly, independent control of central frequency and filter bandwidth over a wide frequency range.

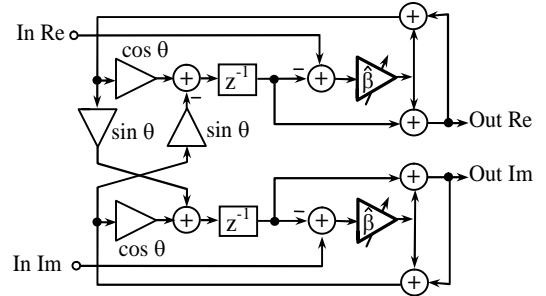


Figure 2. Variable complex BP LS1 filter.

B. Adaptive Complex Filtering

In Figure 3, an adaptive complex notch/BP narrow-band system based on the LS1 variable complex filter is shown [18].

In the following, we consider the input/output relations for corresponding BP/notch filters Eq.(2)-(9). For the BP filter we have the following real output:

$$y_R(n) = y_{R1}(n) + y_{R2}(n), \quad (2)$$

where

$$y_{R1}(n) = -2(2\beta - 1) \cos \theta(n) y_{R1}(n-1) - (2\beta - 1)^2 y_{R1}(n-2) + 2\beta x_R(n) + 4\beta^2 \cos \theta(n) x_R(n-1) + 2\beta(2\beta - 1) x_R(n-2), \quad (3)$$

$$y_{R2}(n) = -2(2\beta - 1) \cos \theta(n) y_{R2}(n-1) - (2\beta - 1)^2 y_{R2}(n-2) - 4\beta(1 - \beta) \sin \theta(n) x_I(n-1). \quad (4)$$

y_R is the real output and x_R is the real input.

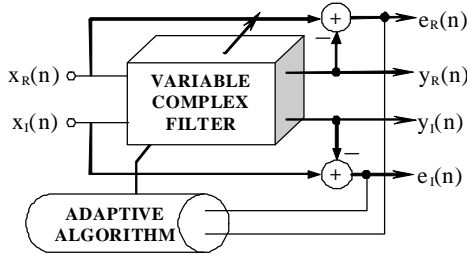


Figure 3. Block-diagram of a BP/notch adaptive complex filter section.

The imaginary output is given by the following equation:

$$y_I(n) = y_{I1}(n) + y_{I2}(n). \quad (5)$$

$$y_{I1}(n) = -2(2\beta - 1) \cos \theta(n) y_{I1}(n-1) - (2\beta - 1)^2 y_{I1}(n-2) + 4\beta(1 - \beta) \sin \theta(n) x_R(n-1), \quad (6)$$

and

$$y_{I2}(n) = -2(2\beta - 1) \cos \theta(n) y_{I2}(n-1) - (2\beta - 1)^2 y_{I2}(n-2) + 2\beta x_I(n) + 4\beta^2 \cos \theta(n) x_I(n-1) + 2\beta(2\beta - 1) x_I(n-2), \quad (7)$$

where y_I is the imaginary output and x_I is the imaginary input.

For the notch filter we have a real output:

$$e_R(n) = x_R(n) - y_R(n), \quad (8)$$

and imaginary output:

$$e_I(n) = x_I(n) - y_I(n). \quad (9)$$

The cost function is the power of the notch filter output signal:

$$[e(n)e^*(n)], \quad (10)$$

where

$$e(n) = e_R(n) + je_I(n). \quad (11)$$

The LMS algorithm is then applied to update the filter coefficient responsible for the central frequency as follows:

$$\theta(n+1) = \theta(n) + \mu \text{Re}[e(n)y'^*(n)]. \quad (12)$$

μ is the step size controlling the speed of convergence, $(*)$ denotes complex-conjugate, $y'(n)$ is the derivative of $y(n) = y_R(n) + jy_I(n)$ with respect to the coefficient subject of adaptation, where

$$y'_R(n) = 2(2\beta - 1) \sin \theta(n) y_{R1}(n-1) - 4\beta^2 \sin \theta(n) x_R(n-1) + 2(2\beta - 1) \sin \theta(n) y_{R2}(n-1) - 4\beta(1 - \beta) \cos \theta(n) x_I(n-1) \quad (13)$$

and

$$y'_I(n) = 2(2\beta - 1) \sin \theta(n) y_{I1}(n-1) + 4\beta(1 - \beta) \cos \theta(n) x_R(n-1) + 2(2\beta - 1) \sin \theta(n) y_{I2}(n-1) - 4\beta^2 \sin \theta(n) x_I(n-1). \quad (14)$$

In order to ensure the stability of the adaptive algorithm, the range of the step size μ should be set according to [21]

$$0 < \mu < \frac{P}{L\sigma^2}. \quad (15)$$

In this case L is the filter order, σ^2 is the power of the signal $y'(n)$ and P is a constant which depends on the statistical characteristics of the input signal. In most practical situations K is approximately equal to 0.1.

This approach can easily be extended to the complex adaptive narrow-band filter bank (Figure 4) [22].

The notch filter bank output signal is described by the following formulae:

$$e_{R_{FB}}(n) = x_R(n) - \sum_{i=1}^M y_{Ri}(n), \quad (16)$$

$$e_{I_{FB}}(n) = x_I(n) - \sum_{i=1}^M y_{Ii}(n), \quad (17)$$

$$e_{FB}(n) = e_{R_{FB}}(n) + je_{I_{FB}}(n), \quad (18)$$

where $M=N_R$ is the number of the receiver's antennae.

The LMS algorithm is applied to adapt the filter bank coefficients [21]:

$$\theta_i(n+1) = \theta_i(n) + \mu \text{Re}[e_{FB}(n)y_i'^*(n)], \text{ for } i = 1 \div M. \quad (19)$$

The main advantages of both the adaptive structure and the filter bank lie in their low computational complexity and fast convergence. The very low sensitivity of the variable complex filter section ensures a high tuning accuracy, even with severely quantized multiplier coefficients and the general efficiency of the adaptation [22].

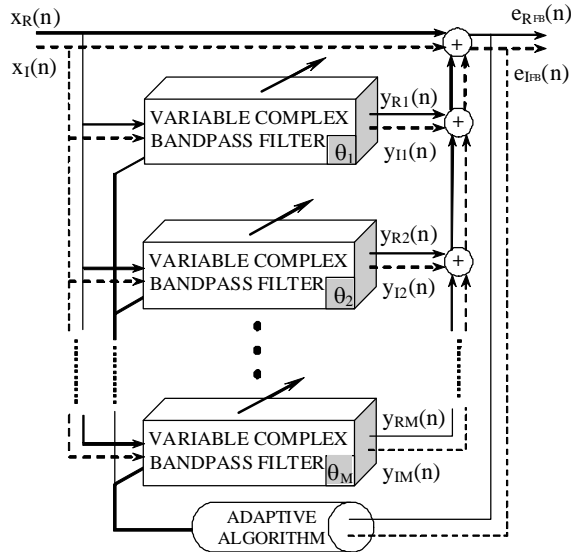


Figure 4. Adaptive complex notch filter bank for the cancellation/enhancement of NBI.

III. SIMULATION MODEL FOR NBI SUPPRESSION IN UWB SYSTEMS

In order to compare the proposed method with other NBI suppression methods, such as Frequency Excision (FE) [23] and Frequency Identification and Cancellation (FIC) [17], a number of simulations relative to complex baseband presentation are performed.

The FE method is applied to the OFDM signal with a complex NBI at the input of the demodulator. The signal is then converted into the frequency domain by FFT, oversampled by 8 and the noise peaks in the spectra of the signal are limited to the determined threshold. The signal is subsequently converted back into the time domain and applied to the input of the demodulator. It should be noted that, for more precise frequency excision, FFT of a higher order than the one in the demodulator is applied.

The FIC method is implemented as a two-stage algorithm. First, the complex NBI frequency is estimated by finding the maximum in the oversampled signal spectrum. Next, using the ML approach, the NBI amplitude and phase are estimated. The second stage realizes the NLS optimization algorithm, where precise estimations of NBI complex amplitude, phase and frequency are performed.

For the realization of the NBI filtering method, the complex adaptive notch filter is connected at the receiver's input. The adaptation algorithm tunes the filter in such a way that its central frequency and bandwidth match the NBI signal spectrum. In the simulations, the central frequency of the notch filter is chosen to be equal to the NBI central frequency, while its bandwidth is equal to 20% of the bandwidth between two adjacent OFDM sub-carriers.

In the OFDM demodulator, the prefix and suffix guard intervals are removed and a 256-point FFT is applied. The pilot tones are removed and a channel equalization of the OFDM symbol is performed. Finally, the corresponding 64-QAM demodulation and decoding is carried out.

The information source is modeled by a generator of uniformly distributed random integers based on the modified version of Marsaglia's "Subtract with borrow algorithm" [24]. The method can generate all the double-precision values in the closed interval $[2^{-53}, 1-2^{-53}]$. Theoretically, this method can generate over 2^{1492} values before repeating itself.

The channel encoder is implemented as a convolutional encoder. In the simulation, the code rate: $R_C = 1/2$ is chosen. In the receiver, a Viterbi hard threshold convolutional decoder is implemented.

A block interleaver-deinterleaver is used in the simulation. The algorithm chooses a permutation table randomly, using the initial state input that is provided.

The digital modulator is implemented as 256-point IFFT. In the OFDM block demodulator, the prefix and suffix guard intervals are removed from each channel and 256-point FFT is also applied. The OFDM symbol consists of 128 data bins and 2 pilot tones. Each discrete piece of OFDM data can use different modulation formats. In the experiments, Grey-encoded 64-QAM modulation format is used. After the IFFT process, the prefix and suffix guard intervals are added.

For the wireless channel, a multi-ray model with direct and delayed (reflected) components is used. The delayed components are subject to fading, while the direct ones are not. To preserve total signal energy, the direct and delayed signal components are scaled by the square roots of $K/(K+1)$ and $1/(K+1)$ respectively. To simplify simulations, a complex baseband representation of the system is used [25] [26].

The NBI is modeled as a single complex tone, the frequency of which is located centrally between two adjacent OFDM sub-carriers.

IV. EXPERIMENTS AND SIMULATION RESULTS

A. NBI Suppression for UWB Channels

Using the above general simulation model, different experiments were performed, estimating the Bit Error Ratio (BER) as a function of the SIR. Four types of channels are considered, i.e., AWGN, CM1, CM2 and CM3 [27] [28]. The CM1, CM2 and CM3 channels are subject to strong fading and additionally background AWGN is applied, so that the signal to AWGN ratio at the input of the OFDM receiver is 20 dB. In Figure 5, a complex AWGN channel is considered. The SIR is varied from -20 dB to 0 dB. It can be seen that for high NBI, where the SIR is less than 0 dB, all methods lead to a significant improvement in performance. The complex adaptive filtering scheme gives better performance than the FE method. This could be explained by the NBI spectral leakage effect caused by DFT demodulation at the OFDM receiver, when many sub-carriers near the interference frequency suffer degradation. Thus, filtering out the NBI before demodulation is better than frequency excision. The FIC algorithm achieves the best result because there is no spectrum leakage, as happens with frequency excision, and there is no amplitude and phase distortion as seen in the adaptive filtering case.

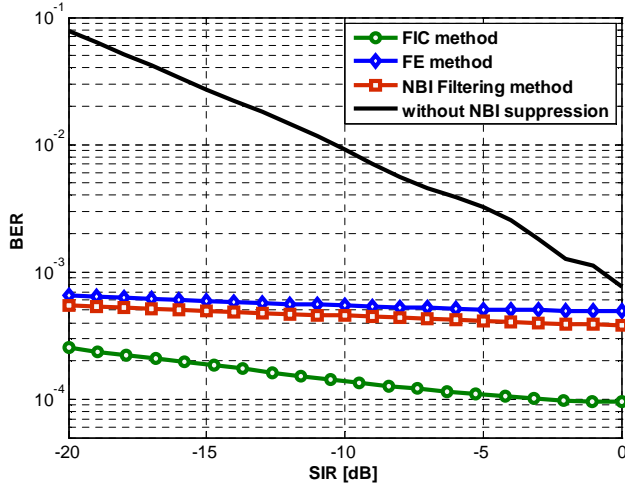


Figure 5. BER as a function of SIR for AWGN channel

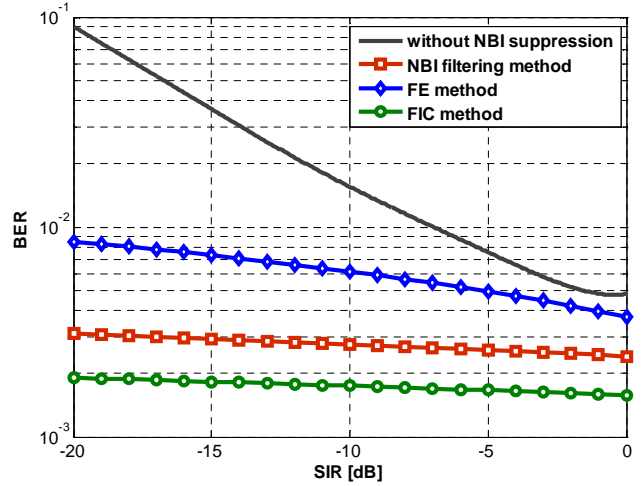


Figure 8. BER as a function of SIR for CM3 channel

In the case of CM1, CM2 and CM3 IEEE UWB channels (Figures 6, 7 and 8) it could be seen that similar results were obtained.

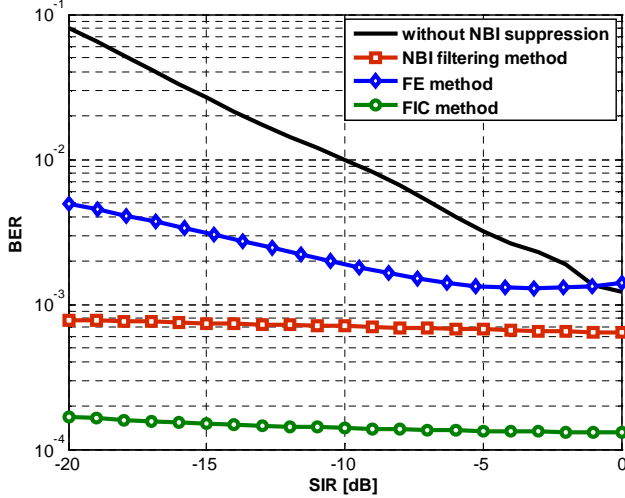


Figure 6. BER as a function of SIR for CM1 channel

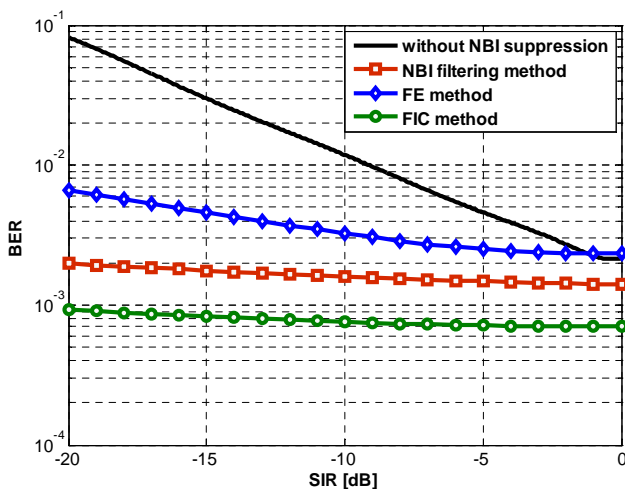


Figure 7. BER as a function of SIR for CM2 channel

It should be noted that the adaptive filtering scheme and frequency cancellation scheme lead to a degradation of the overall performance when $SIR > 0$. This is due either to the amplitude and phase distortion of the adaptive notch filter, or to a wrong estimation of NBI parameters during the identification. The degradation can be reduced by the implementation of a higher-order notch filter or by using more sophisticated identification algorithms. The degradation can be avoided by simply switching off the filtering when $SIR > 0$. Such a scheme is easily realizable as the amplitude of the NBI can be monitored at the BP output of the filter (Figure 3).

In Figure 9, the results of applying a combination of methods are presented. A multi-tone NBI (5 sine-wave interfering signal) is added to the OFDM signal. One of the NBI tones is 10 dB stronger than the others. The NBI filter is adapted to track the strongest NBI tone, thus preventing the loss of resolution and AGC saturation. It can be seen that the combination of frequency excision plus adaptive filtering improves the performance, and the combination of frequency cancellation plus adaptive filtering is even better.

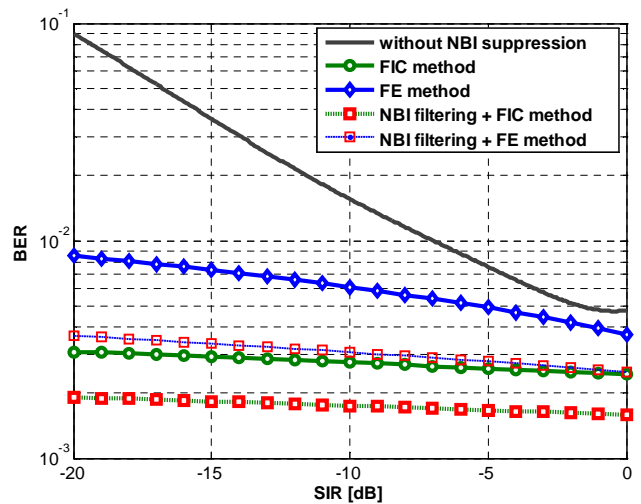


Figure 9. BER as a function of SIR for CM3 channel – multi-tone NBI

Figure 10 shows BER as a function of SIR for the CM3 channel when QPSK modulation is used, the NBI being modeled as a complex sine wave. It can be seen that the relative performance of the different NBI suppression methods is similar to the one in Figure 6 but the BER is higher due to the fact that NBI is QPSK modulated.

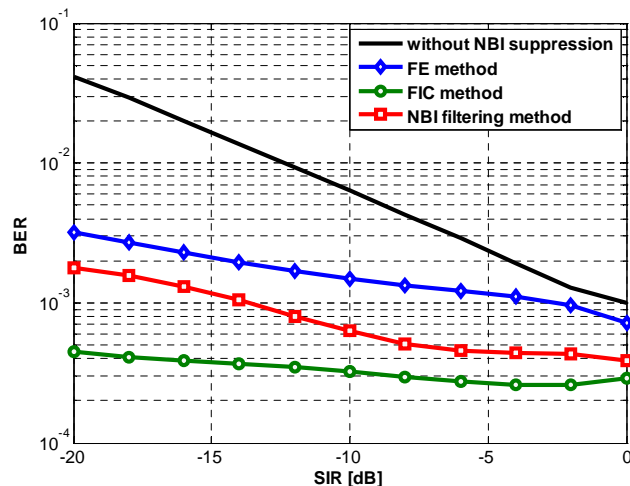


Figure 10. BER as a function of SIR for CM3 channel – QPSK modulated NBI

B. NBI Suppression for MIMO MB-OFDM systems

To evaluate the performance of the three NBI suppression methods, (FE, FIC, and our proposed NBI filtering method), simulations relative to the complex baseband presentation are conducted. A standard MIMO OFDM receiver is assumed and the suppression methods are applied to the MIMO OFDM signal with a complex NBI at each input of the receiver independently.

For the NBI filtering method, the complex adaptive notch filter bank is used. The adaptation algorithm tunes the filter at each receiver input so that its central frequency and bandwidth match the NBI signal spectrum. The Frequency Identification and Cancellation method estimates the complex NBI frequency by determining the maximum in the oversampled signal spectrum per channel.

The OSTBC model for complex signals is realized using the methods described in [29], [30]. The number of transmit antennae N_T can be set from 1 to 4 as long as the number of receive antennae N_R can also be set from 1 to 4. For 2x2 MIMO system, the code rate is $R_c=1$ whereas for 3x3 and 4x4 MIMO systems the code rate is $R_c=1/2$.

The MIMO wireless flat fading channel is realized as given in [31]. A system with N_T transmit antennae and N_R receive antennae is considered. It is assumed that the complex channel gain $h_{i,j}$ is a complex Gaussian random variable: $h_{i,j} \sim \mathcal{N}_c(0,1)$. As the MIMO channel matrix H is not known for the receiver, it must be estimated before the start of the decoding process. The channel estimation method based on the optimal training preamble [31] is adopted. OSTBC decoding, 64-QAM demodulation and error correction decoding are carried out.

Using the above-mentioned simulation model of the Orthogonal Space-Time Block Coding (OSTBC) MIMO system, different experiments were performed to estimate the BER as a function of the SIR. Four types of systems are considered: SISO (1x1), MIMO (2x2), MIMO (3x3) and MIMO (4x4). The MIMO channels are subject to flat fading and, in addition, background AWGN is applied, so that the signal to AWGN ratio at the input of the OFDM receiver is 15dB. In Figure 11, a complex flat fading AWGN channel without NBI suppression is considered. The SIR is varied from -20 dB to 0 dB. It can be seen that 4x4 OSTBC MIMO system gives the best performance.

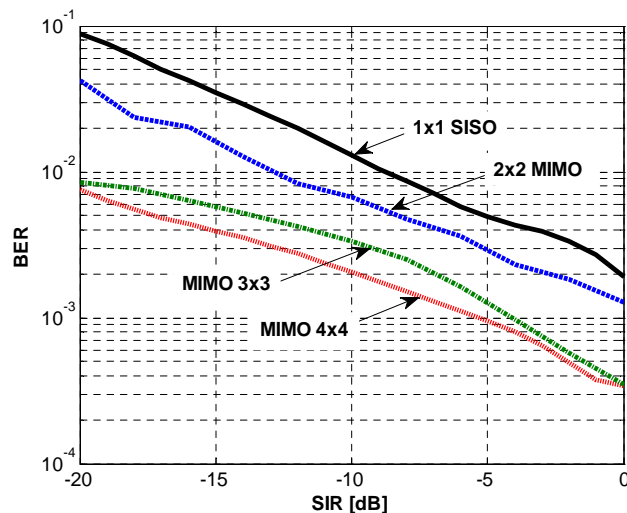


Figure 11. BER as a function of SIR for MIMO channel

Three NBI suppression techniques are then applied: FE, FIC, and the new NBI adaptive filtering method.

In the case of 2x2, 3x3 and 4x4 MIMO channels (Figures 12, 13 and 14) better results in terms of NBI filtering are obtained for higher values of antenna diversity. The FE method manifests good performance for high SIR.

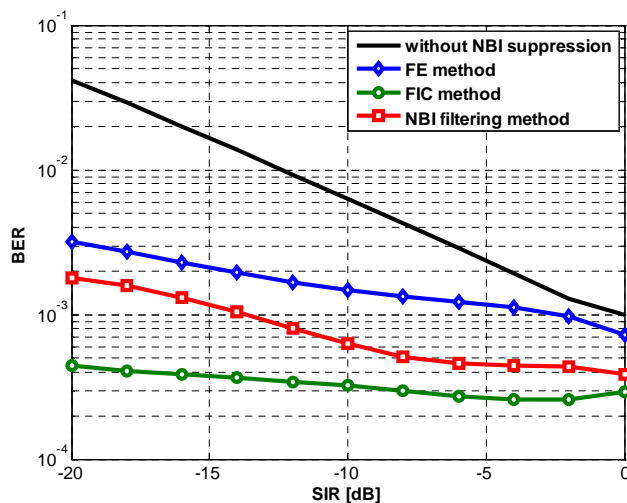


Figure 12. BER as a function of SIR for 2x2 MIMO channel

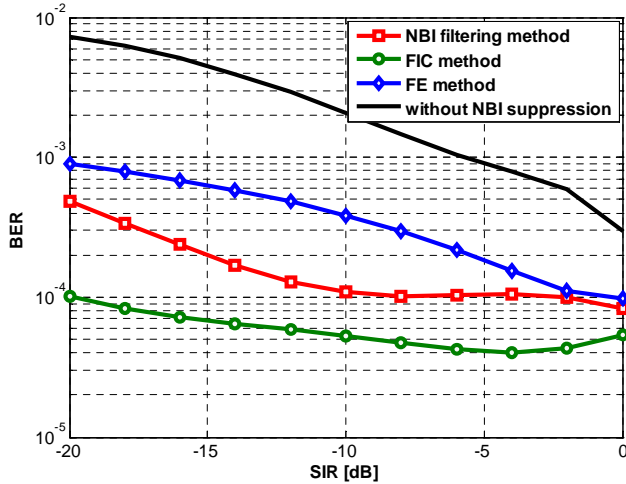


Figure 13. BER as a function of SIR for 3x3 MIMO channel

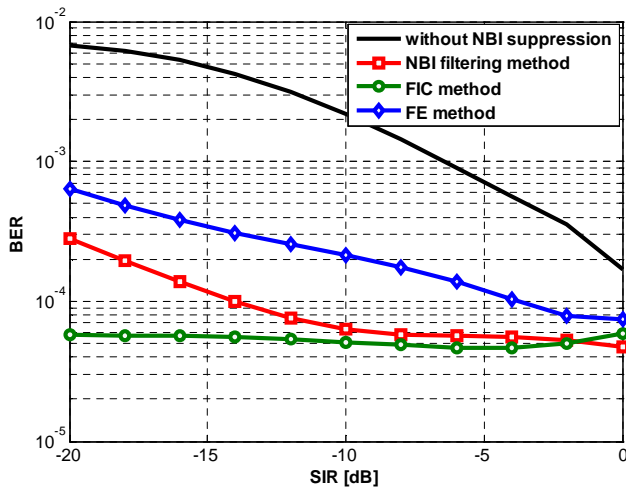


Figure 14. BER as a function of SIR for 4x4 MIMO channel

The experimental results show that the frequency identification and cancellation method achieves the highest performance. On the other hand, the extremely high computational complexity limits its application in terms of hardware resources. In this respect, the adaptive notch filter turns out to be the optimal NBI suppression scheme, as it offers very good performance and reasonable computational complexity. The frequency excision method shows relatively good results and its main advantage is its computational efficiency.

TABLE I. COMPUTATIONAL COMPLEXITY COMPARISON

| Suppression Method | Number of Additions | Number of Multiplications | Complexity |
|---|---------------------|---------------------------|--------------------|
| Frequency Excision | $6MN$ | $4MN\log(N)$ | $\sim O(N\log(N))$ |
| NBI Filtering | KMN | $28MN+KMN^2$ | $\sim O(N^2)$ |
| Frequency Identification and Cancellation | $2MN^2$ | $M(N+2)N^3$ | $\sim O(N^4)$ |

The computational complexity per iteration of the modeled NBI suppression methods are listed in Table I, where: K is a positive integer constant, N is the number of samples to be processed, M is the number of receiver's antennas and $O()$ is the complexity estimation function.

V. CONCLUSIONS

In this paper a method for NBI suppression in MIMO MB-OFDM UWB communication systems, using adaptive complex narrowband filtering, is proposed. In relation to this, a comparison with two other schemes for suppression of complex NBI is performed. The first is a frequency excision method while the second employs frequency identification and cancellation based on ML and NLS algorithms. The experiments show that for high NBI, where the SIR is less than 0 dB, all three suppression methods lead to a significant improvement in performance.

An optimal solution is the adaptive narrowband filtering method, which offers a trade-off between outstanding NBI suppression efficiency and computational complexity. An alternative approach is to implement a combination of the NBI filtering and frequency cancellation methods, thus improving overall performance.

ACKNOWLEDGMENT

This work was supported by the Bulgarian National Science Fund – Grant No. ДО-02-135/2008 “Research on Cross Layer Optimization of Telecommunication Resource Allocation”.

REFERENCES

- [1] M. L. Welborn, “System considerations for ultra-wideband wireless networks,” in IEEE Radio Wireless Conf., Aug. 2001, pp. 5–8.
- [2] J. R. Foerster, “The performance of a direct-sequence spread ultrawideband system in the presence of multipath, narrowband interference, and multiuser interference,” in IEEE Conf. Ultra Wideband Systems Tech., May 2002, pp. 87–91.
- [3] N. Boubaker and K. B. Letaief, “Ultra wideband DSSS for multiple access communications using antipodal signaling,” in IEEE Int. Conf. Commun., vol. 3, May 2003, pp. 11–15.
- [4] E. Saberinia and A. H. Tewfik, “Pulsed and nonpulsed OFDM ultra wideband wireless personal area networks,” in IEEE Conf. Ultra Wideband Systems Tech., Nov. 2003, pp. 275–279.
- [5] A. Batra, J. Balakrishnan, G. R. Aiello, J. R. Foerster and A. Dabak, “Design of a multiband OFDM system for realistic UWB channel environments,” IEEE Transactions Microwave Theory and Techniques, vol. 52, No. 9, pp. 2123–2138, Sep. 2004.
- [6] W. P. Siriwongpairat, M. Olfat, and K. J. R. Liu, “Performance analysis and comparison of time hopping and direct sequence UWB-MIMO systems,” in EURASIP J. Appl. Signal Process. Special Issue on “UWBState of the Art”, vol. 2005, Mar. 2005, pp. 328–345.
- [7] L. Yang and G. B. Giannakis, “Analog space-time coding for multiantenna ultra-wideband transmissions,” IEEE Trans. Commun., vol. 52, no. 3, pp. 507–517, March 2004.
- [8] M. Weisenhorn and W. Hirt, “Performance of binary antipodal signaling over the indoor UWB MIMO channel,” in IEEE Int. Conf. Commun., vol. 4, May 2003, pp. 2872–2878.
- [9] A. Bara, J. Balakrishnan, A. Dabak, R. Gharpurey and J. Lin, “Multi-band OFDM physical layer proposal”, IEEE P802.15-04/0493r1-TG3a, Sept. 2004.

- [10] A. Giorgetti, M. Chiani and M.Z.Win, "The effect of narrowband interference on wideband wireless communication systems", *IEEE Trans. Communications*, vol. 53, No.12, pp. 2139-2149, Dec. 2005.
- [11] Z. Li, A. M. Haimovich, and H. Grebel, "Performance of ultra-wideband communications in the presence of interference," in *Proc. IEEE Int. Conf. Communications*, vol. 10, June 2001, pp. 2948–2952.
- [12] Alan J. Coulson, "Narrowband interference in pilot symbol assisted OFDM systems", *IEEE Trans on Wireless Communications*, vol. 3, No. 6, Nov. 2004, pp. 2277-2287.
- [13] M. Biagi, A. Buccini and L. Taglione, "Advanced methods for ultra wide band receiver design", *Proceedings of the First International Workshop "Networking with UWB"*, Rome, Italy, 21 Dec. 2001.
- [14] C. Carlemalm, H. V. Poor and A. Logothetis, "Suppression of multiple narrowband interferers in a spread-spectrum communication system", *IEEE J. Select. Areas Communications*, vol.3, No. 5, pp. 1431-1436, Sept 2004.
- [15] L. B. Milstein, "Interference rejection techniques in spread spectrum communications", *Proc. IEEE*, vol. 76, No. 6, pp. 657-671, June 1988.
- [16] J. D. Laster and J. H. Reed, "Interference rejection in digital wireless communications", *IEEE Signal Proc. Mag.*, vol. 14, No. 3, pp. 37 – 62, May 1997.
- [17] E. Baccarelli, M. Baggi and L. Taglione, "A novel approach to in-band interference mitigation in ultra wide band radio systems", *IEEE Conference on Ultra Wide Band Systems and Technologies*, 2002.
- [18] G. Iliiev, Z. Nikolova, G. Stoyanov and K. Egiazarian, "Efficient design of adaptive complex narrowband IIR filters", *Proceedings of XII European Signal Processing Conference, EUSIPCO 2004*, Vienna, Austria, pp. 1597 - 1600, 6 - 10 Sept. 2004.
- [19] S. Y. Park, G. Shor, and Y. S. Kim, "Interference resilient transmission scheme for multi-band OFDM system in UWB channels," in *Proc. IEEE Int. Circuits and Systems Symp.*, vol. 5, Vancouver, BC, Canada, May 2004, pp. 373–376.
- [20] G. Stoyanov, M. Kawamata and Z. Valkova, "New first and second-order very low-sensitivity bandpass/bandstop complex digital filter sections", *Proc. IEEE Region 10th Annual Conf. "TENCON'97"*, Brisbane, Australia, vol. 1, Dec. 2-4, 1997, pp. 61-64.
- [21] S. Douglas, "Adaptive filtering, in digital signal processing handbook", D. Williams and V. Madiseti, Eds., Boca Raton: CRC Press LLC, pp. 451-619, 1999.
- [22] Z. Nikolova, G. Iliiev, G. Stoyanov and K. Egiazarian, "Design of adaptive complex IIR notch filter bank for detection of multiple complex sinusoids", *Proc. International Workshop SMMSP'2002*, Toulouse, France, pp. 155-158, Sept. 2002.
- [23] J.-C. Juang, C.-L. Chang and Y.-L. Tsai, "An interference mitigation approach against pseudolites", *The 2004 International Symposium on GNSS/GPS*, Sydney, Australia, 6 – 8 Dec. 2004.
- [24] S. Tezuka, P. L'Ecuyer and R. Couture, "On the lattice structure of the add-with-carry and subtract-with-borrow random number generators", *ACM Transactions on Modeling and Computer Simulation (TOMACS)*, vol. 3, Issue 4, pp. 315 – 331, Oct. 1993.
- [25] R. van Nee and R. Prasad, *OFDM for wireless multimedia communications*, Artech House, 2000.
- [26] H. Schulze and C. Luders, *Theory and applications of OFDM and CDMA*, John Wiley, 2005.
- [27] M.-O. Wessman, A. Svensson and E. Agrell, "Frequency diversity performance of coded multiband-OFDM systems on IEEE UWB Channels", *COST 289 Workshop*, Gothenburg, Sweden, April 2007.
- [28] A. F. Molisch and J. R. Foerster, "Channel models for ultra wideband personal area networks", *IEEE Wireless Communications*, pp. 524-531, Dec. 2003.
- [29] S. Alamouti, "Simple transmit diversity technique for wireless communications", *IEEE Journal Select. Areas Commun*, vol. 16, No. 8, pp. 1451–1458, Oct. 1998.
- [30] I. Berguer and Dong, "Space-time coding and signal processing for MIMO communications", *J Comput. Sci & Technol.*, vol. 18, No 6, pp. 689-702, Nov. 2003.
- [31] M. Ovtcharov, V. Poulkov, G. Iliiev and Z. Nikolova, "Narrowband interference suppression for IEEE UWB channels", *Proc. ICDDT 2009*, Colmar, France, pp. 43-47.